COMBINATION OF ELECTRIC AND MAGNETIC DIPOLES WITH SINGLE ELEMENT FEEDING FOR BROADBAND APPLICATIONS

Karlo Q. da Costa[1], and Victor Dmitriev[1]

[1]Department of Electrical Engineering and Computation, Federal University of Para

Av. Augusto Corrêa nº 01, CEP 66075-900, Belém-PA, Brazil

ABSTRACT: *This work presents four types of broadband compound antennas. The antennas are a combination of an electric dipole and small square or circular loops. The feeding of the electric dipole only is realized. The input impedance, the reflection coefficient and the gain of the antennas with different geometries are analyzed numerically by the method of moments. It is shown that for the level of the reflection coefficient $|\Gamma|<-10$dB, the (80-90)% bandwidth of the proposed antennas can theoretically be achieved.*

Key words: *Electric and magnetic dipoles; broadband antennas; combined antennas.*

Karlo Q. da Costa (e-mail: karlocosta@yahoo.com.br)

Victor Dmitriev (e-mail: victor@ufpa.br)

I. INTRODUCTION

General fundamental limits about performance of antennas were for the first time investigated by Wheeler [1] and Chu [2]. They showed in particular that an antenna possesses the minimum radiation factor if and only if this antenna radiates the fundamental modes TM_{10} and TE_{10} with equal amount of energy. These modes are radiated by the infinitesimal electric and magnetic dipoles, respectively [3]. More recent works that confirm this conclusion can be found in [4, 5]. Notice that the radiation factor is inversely proportional to the bandwidth of the antenna.

The results of this general theory suggest combining electric and magnetic dipoles to increase the bandwidth. Investigations on the mutual interaction between an electrical dipole and a magnetic dipole (small loop) for different relative orientations of their dipole moments are presented in [6, 7]. The authors of [7] adjusted the magnitudes of currents of the dipoles with the purpose to obtain equal power of the TE and TM modes. They noted a significant absorption of energy by one of the active dipoles when the dipole moments are orthogonal.

In [8], a combination of one electric dipole and two magnetic dipoles with sinusoidal distribution of the electric and magnetic currents along the dipoles was used. The authors of the paper obtained broadband characteristics adjusting positions of the elements and magnitudes and phases of currents of the sources. However, the realization of this antenna is not simple because the theory supposes the ideal magnetic dipole, and the optimal magnitudes and phases of the sources depend on frequency.

The main idea of our paper is to use several coupled radiating elements and to vary the mutual positions of them in order to enlarge the bandwidth of the combined antenna. In contrast to [8], all of the antennas presented here are combinations of orthogonal electric and magnetic dipoles (in fact, circular or square loops) with feeding of the electric dipole only. Thus, it is not

required to control the magnitudes and phases of the sources in function of frequency, and the absorption in the passive elements is decreased. The input impedance, reflection coefficient and gain for these antennas were calculated by the Method of Moments (MoM) [9]. The description of the antennas is given in Section II. Section III presents the numerical results and their analysis and Section IV contains the conclusions.

II. DESCRIPTION OF THE ANTENNAS

The geometries of the four analyzed antennas are shown in Figure 1. These antennas consist of a combination of one electric dipole and one or two loops. The small loops can be considered as magnetic dipoles. All the elements are put close to each other (but without electric contact) in order to obtain near field coupling between them.

In all these configurations, the electric current source is connected in the middle of the electric dipole. Thus, the electric dipole is the driving element. The loops are passive elements. In Figure 1, square loops are shown. For comparison, the loops of the circular form are also analyzed. The diameter of the circular loop is chosen to be equal to the side of the corresponding square loop.

In Figure 1, L_d represents the length of the electric dipole and L_l is a side of the square loop (or the diameter of the circular loop). In all the four cases of Figure 1, the electric dipole is oriented along the axis z. This dipole is symmetrical with respect to the point z=0. A combination of one electric dipole and one loop is depicted in Figure 1(a). The loop is in the plane $y=d_1$ with its center in the point x=0, z=0. Thus, the magnetic moment of the loop is oriented along the axis y.

Figure 1(b) shows also a combination of one electric dipole and one loop, but the loop in this case is in the plane xz (x>0) so that the magnetic moment of the loop is orthogonal to the

plane *xz*. The loop is placed symmetrically with respect to the axis *x*. The smallest distance between the two radiating elements in Figure 1(b) is denoted by d_2.

In Figure 1(c) and Figure 1(d), there are two loop elements. In Figure 1(c), the loops are in the plane *xz* and they are symmetric with respect to the origin and the axis *x*. The smallest distance between the loops and the electric dipole is d_3. In the second case showed in Figure1(d), the loops are in the plane *xz* ($x>0$), and they are symmetric with respect to the axis *x*. The smallest distance between the loops and the axis *x* is d_4, and the smallest distance between the loops and the electric dipole is d_5.

In all the cases showed in Figure 1, the electric and magnetic dipole moments are orthogonal. Such a choice of the mutual orientation of the dipoles will be discussed below.

III. NUMERICAL RESULTS

The numerical results presented here were obtained by MoM codes that we developed to analyze the four antennas showed in Figure 1. In these codes, we employed pulse and Dirac's delta functions for basis and test functions, respectively. In all simulations, we used 15, 20 and 16 segments of discretization for the electric dipole, square loop and circular loop, respectively.

A. Mutual Impedance between Electric and Magnetic Dipoles. The influence of a passive magnetic dipole on the characteristics of the combined antenna depends on coupling between the electric and magnetic dipoles. Mathematically, this coupling can be described by an impedance matrix [*Z*]. In order to analyze the mutual impedance between electric and magnetic dipoles with different orientation, we considered two extreme cases. In the first one, the moments of the dipoles are aligned along the axis *z* (Figure 2(a)). The source 1 is connected in the middle of the electric dipole and the source 2 is in the middle of a side of the square loop.

In the second case on Figure 2(b), the moments are orthogonal. The electric dipole is on the axis z and the square loop is in the plane xz. This case corresponds to the combined antenna shown in Figure 1(a) with d_1=0. In this case the source 2 is set in the point $x=L_l/2$ and z=0. The geometrical dimensions in these two configurations are L_d=0.02λ, L_l=0.025λ where λ is the wavelength. The radius of the circular conductor of the electric dipole and the loop is a=0.001λ.

The numerical results for the elements of the 4x4 impedance matrix [Z] between the ports 1 and 2 for the two combinations of electric and magnetic dipoles are presented in Table 1. The results obtained by other researchers [6, 7] are also given in this table for comparison. We can see from this table that the coupling between the dipoles is nearly zero ($Z_{12} \approx Z_{21} \approx 0$) when the moments are aligned. For the case of the orthogonal orientation of the moments (Figure 2(b)), the values of Z_{12} e Z_{21} are considerable. This property predetermined our choice of the mutual orientation of the electric and magnetic dipoles.

TABLE 1 Elements of the Impedance Matrix for Electric and Magnetic Dipoles (Ohms)

	Obtained here	Obtained in [6]	Obtained in [7]
		Aligned dipole moments	
Z_{11}	4.5×10^{-2}–j2.1×10^{3}	5.2×10^{-2}–j2.4×10^{3}	4.5×10^{-2}–j2.3×10^{3}
Z_{12}	8.8×10^{-21}+j9.7×10^{-17}	-8.2×10^{-14}+j2.7×10^{-14}	6.2×10^{-17}–j4.2×10^{-15}
Z_{21}	1.5×10^{-19}+j1.2×10^{-15}	-1.1×10^{-12}–j1.2×10^{-12}	4.3×10^{-20}–j1.2×10^{-15}
Z_{22}	1.4×10^{2}+j9.4×10^{1}	1.4×10^{2}+j9.8×10^{1}	1.4×10^{-2}+j9.8×10^{1}
		Orthogonal dipole moments	
Z_{11}	3.5×10^{-3}–j2.0×10^{3}	4.8×10^{-3}–j2.2×10^{3}	4.5×10^{-3}–j2.1×10^{3}
Z_{12}	3.3×10^{-4}+j1.2×10^{1}	1.4×10^{-4}+j1.3×10^{1}	1.0×10^{-4}+j1.2×10^{1}
Z_{21}	3.3×10^{-4}+j1.2×10^{1}	1.1×10^{-4}+j1.3×10^{1}	1.0×10^{-4}+j1.2×10^{1}
Z_{22}	1.4×10^{-2}+j9.4×10^{1}	1.4×10^{-2}+j9.8×10^{1}	1.4×10^{-2}+j9.8×10^{1}

B. Input Impedance. For the four types of antennas in Figure 1, we have calculated the frequency dependence of the input impedance of the antennas changing the dimensions L_l, d_1, d_2, d_3, d_4 e d_5 (the dimensions are normalized with L_d) for different forms of the loops (square or circular). The radius of the circular conductors used in all our simulations was fixed by the value $a=L_d/200$. The losses in the conductors were neglected. The frequency range of our calculations is $0.3<L_d/\lambda<2$.

The largest bandwidths were obtained for the antennas with the following parameters:

Case 1: $L_l/L_d=0.25$ and $d_1/L_d=0.03$, circular loop.

Case 2: $L_l/L_d=0.30$ and $d_2/L_d=0.03$, square loop.

Case 3: $L_l/L_d=0.25$ and $d_3/L_d=0.04$, square loop.

Case 4: $L_l/L_d=0.25$, $d_4/L_d=0.02$ and $d_5/L_d=0.02$, circular loop.

The plots of the input impedance $Z_{in}=R_{in}+jX_{in}$ for the best results are shown in Figures 3, 4, 5 and 6. For comparison, the input impedance of the single electric dipole with the dimensions L_d and $a=L_d/200$ is also depicted in these figures.

C. Reflection Coefficient and Gain. For the antennas with the characteristics shown in Figures 3, 4, 5 and 6, we have also calculated the reflection coefficient $|\Gamma|=|(Z_{in}-Z_0)/(Z_{in}+Z_0)|$ and the gain $G=U/U_0$, where Z_0 is the impedance of the feeding transmission line, U and U_0 are the radiation intensity of a compound antenna and the isotropic radiator, respectively. Figures 7, 8, 9 and 10 demonstrate the frequency dependence of $|\Gamma|$ and G (in dB) for these antennas. The gain shown in these figures is only the G_θ component in the directions $+x$, $+y$, $-x$ and $-y$ ($G_\phi=0$ for this

antennas). The directions for which these gains were calculated depend on the symmetry of each combined antenna. In our calculations, the values of the transmission line impedance Z_0 were chosen 320, 210, 250 and 300 Ohms for the Cases 1, 2, 3 and 4, respectively. Figures 7, 8, 9 and 10 show also the values of $|\Gamma|$ for the single electric dipole with $a=L_d/200$, $Z_0=73$ Ohms. The bandwidth of the single electric dipole is 12,2%.

Table 2 gives the values of the bandwidth B of the antennas ($B=2(f_s-f_i)/(f_s+f_i)\times 100\%$, where f_s and f_i are the superior and inferior frequencies, respectively, for the level $|\Gamma|=-10$dB). This table gives also the normalized wavelength L_d/λ_c, where λ_c is the wavelength corresponding to the central frequency $f_c=(f_s+f_i)/2$.

In Figures 7, 8, 9 and 10, the values of $|\Gamma|$ in the frequency range $f_i<f<f_s$ vary between –15dB and –10dB. Case 1 is an exception (Figure 7), where we have $|\Gamma|<-15$dB for $L_d/\lambda \approx 1.4$, and also Case 2 (Figure 8) where $|\Gamma|<-15$dB for $L_d/\lambda \approx 0.9$. Better results for the parameter $|\Gamma|$ in these ranges can be obtained adjusting the dimensions and positions of the loop antennas, but these improved values of $|\Gamma|$ lead to a smaller bandwidth. Typical values of B obtained in all our simulations are in the range $30<B(\%)<50$ and the values of the feeding line impedances are in the range $140<Z_0(\text{Ohms})<400$.

Thus, we can improve the input matching adjusting the antenna's dimensions but at the expense of the bandwidth. To demonstrate this statement, we present in Figure 11 the values of $|\Gamma|$ of the antenna for Case 4 with square loops with the parameters $L_l/L_d=0.225$, $d_4/L_d=0.05$ and $d_5/L_d=0.02$. This antenna has a smaller bandwidth in comparison with the antenna in Figure 10, but its bandwidth ($B=55.6\%$) is larger then the bandwidth of the antennas presented in [10] ($B=17\%$) where the authors used combinations of the electric dipoles only.

TABLE 2 Bandwidth *B* of the Antennas

	Loop	B (%)	Z_0 (Ohms)	L_d/λ_c
Case 1	Circular	84.18	320	1.1541
Case 2	Square	54.05	210	0.7437
Case 3	Square	59.41	250	0.8358
Case 4	Circular	86.04	300	1.1625

IV. CONCLUSIONS

We have presented in this work some preliminary results concerning the antennas combined of electric and magnetic dipoles with single feeding that possess an increased bandwidth. The electromagnetic coupling between the orthogonal electric and magnetic dipoles modifies the input impedance of the antenna. Varying the loop antenna's dimensions and their positions with respect to the electric dipole, it is possible to obtain better input matching in comparison with the isolated electric dipole and a combination of the electric dipoles, and consequently, larger bandwidth. These rather simple antennas can theoretically achieve the bandwidth of (80-90)%. Applying some optimization techniques, such as for example genetic algorithm, we hope to improve further the frequency characteristics of such antennas.

ACKNOWLEDGMENT

This work was supported by the Brazilian agency CNPq.

REFERENCES

1. H. A. Wheeler, Fundamental limitations of small antenna, Proc. IRE, Vol. 35, December 1947, pp. 1479-1484.
2. L. J. Chu, Physical limitations of omni-directional antennas, J. Appl. Phys., Vol. 19, December 1948, pp. 1163-1175.
3. J. S. McLean, A re-examination of the fundamental limits on the radiation Q of electrically small antennas, IEEE Trans. Ant. Propag., Vol. 44, N5, May 1996, pp. 672-675.
4. W. Geyi, P. Jarmuszewski, Y. Qi, The foster reactance theorem for antennas and radiation Q, IEEE Trans. Ant. Propag., Vol. 48, N3, March 2000, pp. 401-408.
5. W. Geyi, Physical limitations of antenna, IEEE Trans. Ant. Propag., Vol. 51, N8, August 2003, pp. 2116-2123.
6. J. S. McLean, The application of the method of moments to the analysis of electrically small "compound" antennas, IEEE Int. Symp. on Electromag. Compat., August 1995, pp. 119-124.
7. F. Tefiku, C. A. Grimes, Coupling between elements of electrically small compound antennas, Microwave and Optical Technology Letters, Vol. 22, July 1999, N1, pp. 16-21.
8. V. P. Belichenko, Y. I. Buyanov, V. I. Koshelev, V. V. Plisko, On the possibility of extending the passband of small-size radiators, J. of Commun. Techn. and Electronics, Vol. 44, N2, 1999, pp. 167-172.
9. R. F. Harrington, Field computation by moment method, Macmillan: New York, 1968, pp. 62-81.
10. T. Fukasawa, H. Ohmine, K. Miyashita, Y. Chatani, Triple-bands broad bandwidth dipole antenna with multiple parasitic elements, IEICE Trans., Vol. E84-B, N9, September 2001, pp. 2476-2481.

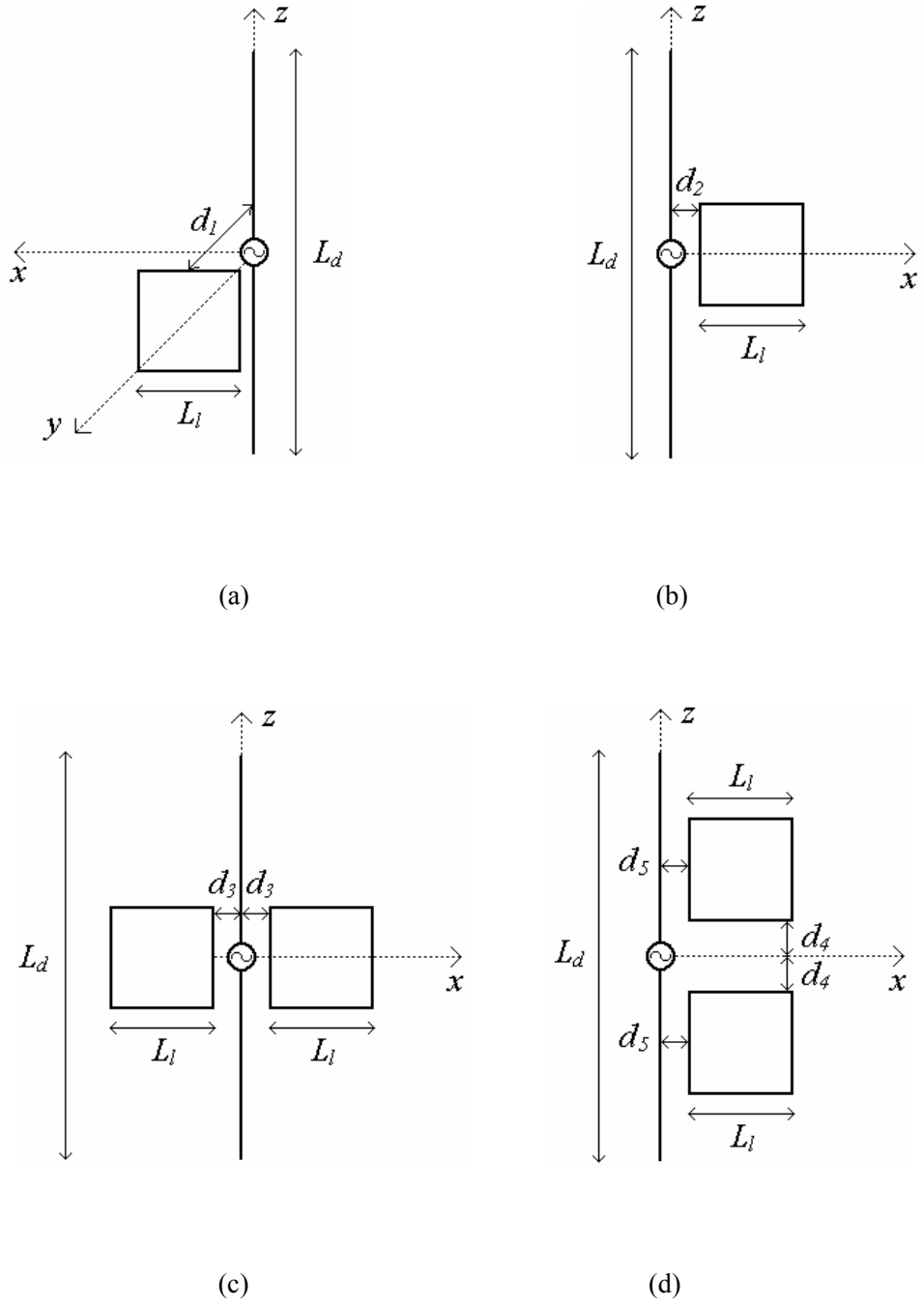

Figure 1 Four types of the analyzed antennas. (a) Case 1. (b) Case 2. (c) Case 3. (d) Case 4.

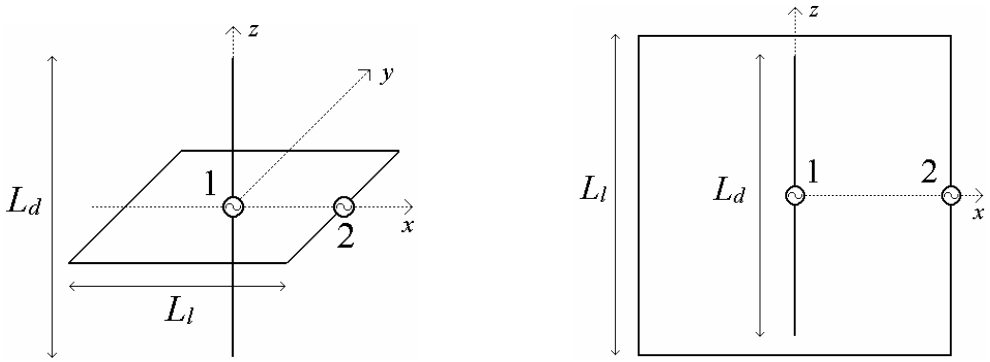

(a) (b)

Figure 2 Combinations of electric and magnetic dipoles with different orientation of their moments. (a) aligned dipole moments. (b) orthogonal dipole moments.

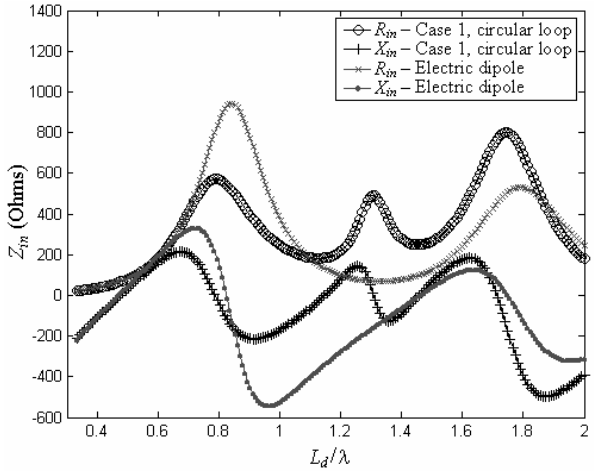

Figure 3 Input impedances of the compound antenna for Case 1, and for the single electric dipole.

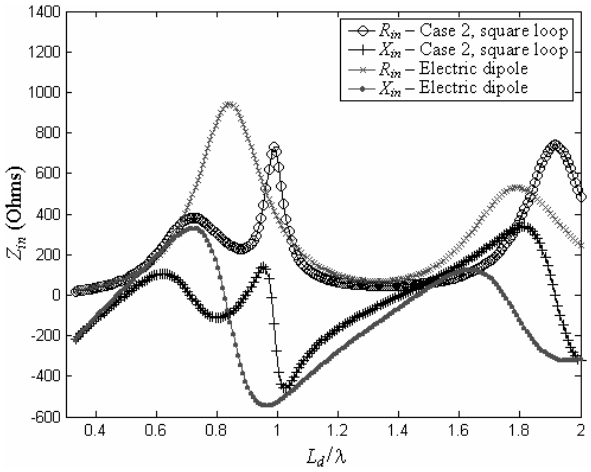

Figure 4 Input impedances of the compound antenna for Case 2, and for the single electric dipole.

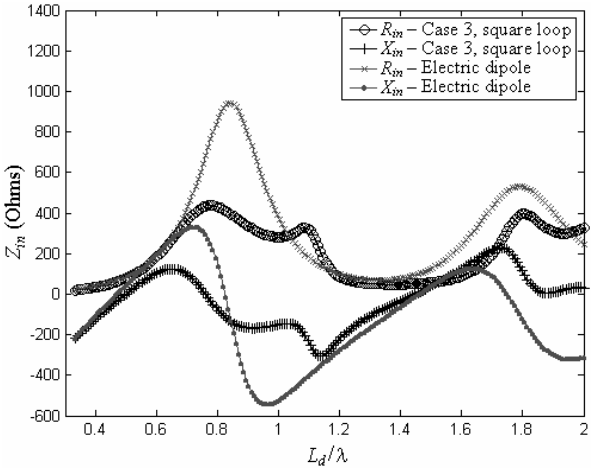

Figure 5 Input impedances of the compound antenna for Case 3, and for the single electric dipole.

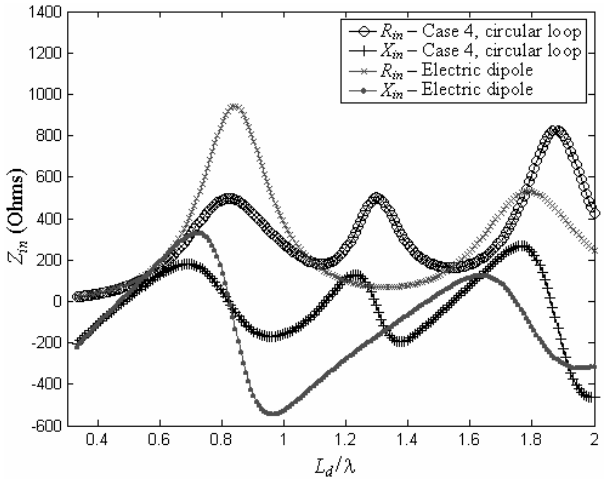

Figure 6 Input impedances of the compound antenna for Case 4, and for the single electric dipole.

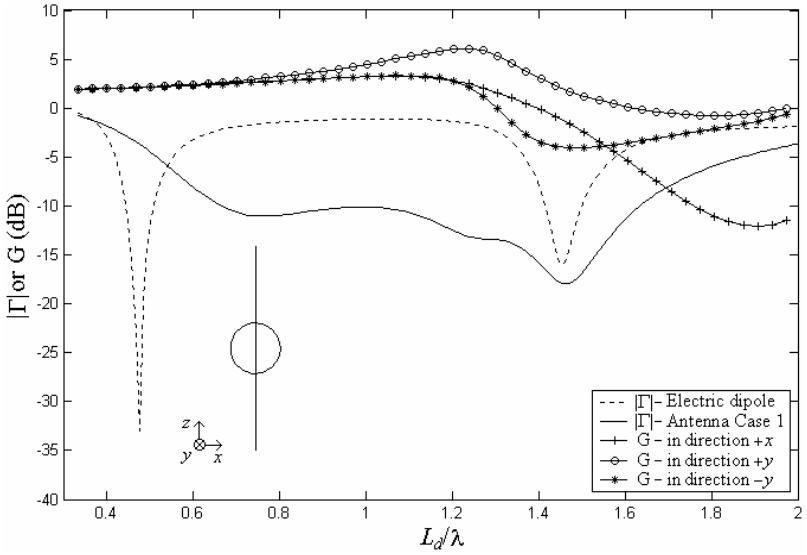

Figure 7 Reflection coefficient |Γ| and gain G of the antenna for Case 1, and for the single electric dipole.

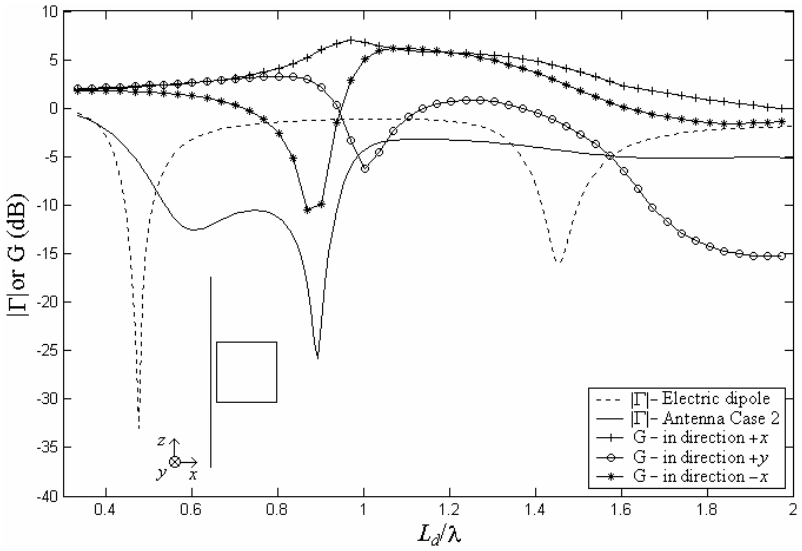

Figure 8 Reflection coefficient |Γ| and gain G of the antenna for Case 2, and for the single electric dipole.

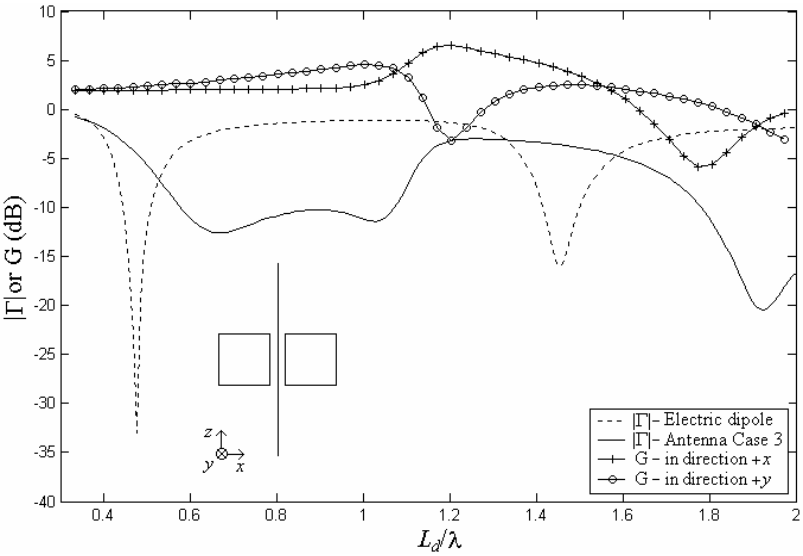

Figure 9 Reflection coefficient |Γ| and gain G of the antenna for Case 3, and for the single electric dipole.

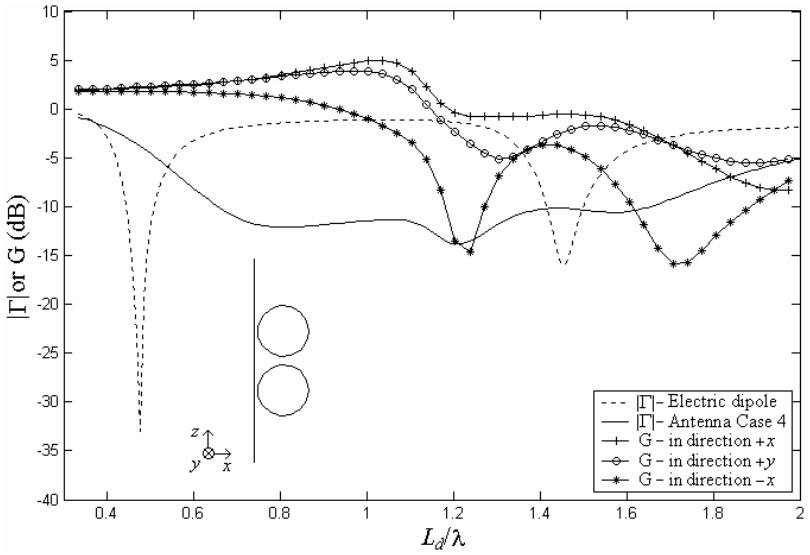

Figure 10 Reflection coefficient |Γ| and gain G of the antenna for Case 4, and for the single electric dipole.

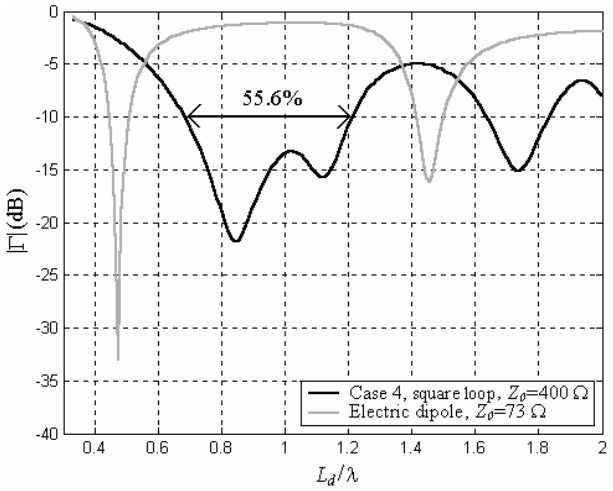

Figure 11 Reflection coefficient |Γ| of the antenna for Case 4, and for the single electric dipole.